Published in final edited form as:
J Neuroimmunol. 2008 December 15; 205(1-2): 94–100. doi:10.1016/j.jneuroim.2008.09.013.

PrP Antibody Binding-Induced Epitope Modulation Evokes Immunocooperativity

Binggong Chang[1], **Michael W. Miller**[2], **Marie S. Bulgin**[3], **Sharon Sorenson-Melson**[3], **Aru Balachandran**[4], **Allen Chiu**[1], and **Richard Rubenstein**[1,*]

1 *Department of Biochemistry, SUNY Downstate Medical Center, 450 Clarkson Avenue, Brooklyn, NY 11203, USA*

2 *Colorado Division of Wildlife, Wildlife Research Center, 317 West Prospect Road, Fort Collins, CO 80526-2097, USA*

3 *University of Idaho, Caine Veterinary Teaching and Research Center, 1020 E. Homedale Road, Caldwell, ID 83605, USA*

4 *Animal Diseases Research Institute, Canadian Food Inspection Agency, 3851 Fallowfield Road, Nepean, Ontario, K2H 8P9, Canada*

Abstract

We have characterized the antibody-antigen binding events of the prion protein (PrP) utilizing three new PrP-specific monoclonal antibodies (Mabs). The degree of immunoreactivity was dependent on the denaturation treatment with the combination of heat and SDS resulting in the highest levels of epitope accessibility and antibody binding. Interestingly however, this harsh denaturation treatment was not sufficient to completely and irreversibly abolish protein conformation. The Mabs differed in their PrP epitopes with Mab 08-1/11F12 binding in the region of $PrP_{93–122}$, Mab 08-1/8E9 reacting to $PrP_{155–200}$ and Mab 08-1/5D6 directed to an undefined conformational epitope. Using normal and infected brains from hamsters, sheep and deer, we demonstrate that the binding of PrP to one Mab triggers PrP epitope unmasking, which enhances the binding of a second Mab. This phenomenon, termed positive immunocooperativity, is specific regarding epitope and the sequence of binding events. Positive immunocooperativity will likely increase immunoassay sensitivity since assay conditions for PrP^{Sc} detection does not require protease digestion.

Keywords

Prion protein; Monoclonal antibodies; Epitope recognition; Immunocooperativity

1. Introduction

Prion diseases, also known as transmissible spongiform encephalopathies (TSEs), are invariably fatal neurodegenerative disorders affecting a broad spectrum of host species and arise via genetic, infectious, or sporadic mechanisms. In humans, prion diseases consist of

*Please send all proofs and correspondence to: Dr. Richard Rubenstein, SUNY Downstate Medical Center, Department of Biochemistry, Box #8, 450 Clarkson Avenue, Brooklyn, NY 11203, Tel: 718 270-2019, Fax: 718 270-2459, Email: richard.rubenstein@downstate.edu.

various forms of Creutzfeldt-Jakob disease (sporadic, familial, iatrogenic, variant), Gerstmann-Straussler-Scheinker syndrome, Kuru and Fatal Familial Insomnia Prion diseases in animals include scrapie in sheep, bovine spongiform encephalopathy (BSE) in cattle and chronic wasting disease (CWD) in deer and elk. (Glatzel et al., 2003; Collins et al., 2004; Prusiner, 1998; Abid and Soto, 2006; Wadsworth and Collinge, 2007)

Regardless of the data supporting or refuting the prion (Prusiner, 1982), virino (Dickinson and Outram, 1988) and virus (for review see Manuelidis, 2007) theories of the nature of the infectious agent, a key event in prion diseases is the accumulation of an abnormal isoform (PrP^{Sc}) of a host-encoded protein, termed prion protein (PrP^{C}), predominantly in the nervous system of the infected host (Stahl et al., 1993). Structurally, PrP consists of a disordered, flexible amino terminal region comprising approximately residues 23–124 and a globular carboxyl terminal domain (approximately residues 125–231). The carboxyl terminal region is directly associated with the formation of fibrils and aggregates associated with the disease. The amino terminal region is involved in protein structural stability and the folding of PrP^{C} to PrP^{Sc} (Cordeiro et al., 2005). PrP^{C} and PrP^{Sc} differ in their sensitivities to proteinase K (PK) with PrP^{C} being completely digested and PrP^{Sc} converted to a protease resistant core (PrP27-30) comprising approximately the PrP residues 90–231. PrP^{C} and PrP^{Sc} also differ in their secondary and tertiary structures (Basler et al., 1986; Caughey et al., 1991; Stahl and Prusiner, 1991; Caughey and Raymond, 1991; Pan et al., 1993; Kocisko et al., 1994; 1995). Fourier transform infrared (FTIR) and circular dichroism spectroscopy studies indicate that PrP^{C} is highly helical (42%) with little β-sheet structure (3%) (Pan et al., 1993). In contrast, PrP^{Sc} contains less helical structure (30%) and a large amount of β-structure (43%). PrP^{C} can be converted to the lethal PrP^{Sc} conformation on contact with PrP^{Sc}(Horiuchi and Caughey, 1999; Safar et al., 1998; Caughey, 2001). Several mechanisms have been proposed for the spontaneous and/or assisted conversion of endogenous PrP^{C} to PrP^{Sc} (Caughey, 2001). A confounding factor in conversion is that PrP^{Sc} is conformationally heterogeneous (Cohen and Prusiner, 1998) which suggests a degree of structural flexibility.

PrP^{Sc} represents the only disease-specific macromolecule identified to date, and the majority of testing procedures are based on the proteolytic removal of endogenous PrP^{C} followed by the immunological detection of PrP^{Sc}. The degree of resistance of PrP^{Sc} to proteolysis is likely related to the amount of PK used for digestion as well as factors associated with PrP^{Sc} including concentration, state of aggregation, unique conformation and other molecules. Such assays become problematic when PrP^{Sc} is present only in low amounts as the enzyme may digest it. On the other hand, it is important to use sufficient PK to digest all of the PrP^{C} that is present to eliminate the possibility of false positive results. Confounding this issue is the concept of PK-sensitive PrP^{Sc} ($sPrP^{Sc}$) (Safar et al., 1998) that has been reported to constitute the majority of PrP^{Sc} in the brains of individuals who had died from CJD (Safar et al., 2005). Therefore, the use of PK likely results in an underestimate of the total PrP^{Sc} present in a sample. This becomes an important issue in the development of a prion disease-specific ante-mortem assay using biological fluids where the levels of PrP^{Sc} are presumably very low. The development of diagnostic assays that do not require proteolytic treatment of samples would eliminate the issues associated with proteolytic digestion and reduced assay sensitivity.

Molecular dynamic simulations provide information about the conversion process as well as possible PrP^{Sc} models and illustrate the complexities involved in the conversion of PrP and in developing diagnostics for PrP^{Sc} (Alonso et al., 2001; 2002). In extreme examples the surface of one form of the protein can change dramatically so that epitopes found in one form of PrP are unavailable for binding in another form (e.g., the monoclonal antibody [Mab] 3F4 epitope is less accessible in the PrP^{Sc} form; Peretz et al., 1997).

Furthermore, previous studies have shown that the binding of an antibody specific for the N terminus of PrP^{C} can block the recognition of another antibody that normally binds to a conformational epitope located within the C terminus. It is likely that the binding of the first antibody causes a specific, but subtle, conformational change within the C terminus resulting in a loss or masking of the epitope of the second antibody (Li et al., 2000). This concept, which we refer to as negative immunocooperativity, describes the loss of antibody binding to its epitope resulting from a change in the antigen which was induced by the initial binding of a different antibody to its specific epitope.

In this paper, we describe dynamic antibody-antigen interactions resulting in positive prion protein immunocooperativity. We hypothesize that this event consists of PrP^{Sc} spatial rearrangement, which may also be associated with non-PrP macromolecular denaturation, resulting in PrP epitope unmasking. This finding has important implications for PrP structural analysis, detection of PrP^{Sc} without proteolysis resulting in enhancing PrP^{Sc} assay sensitivity, and targeting specific PrP sites for therapeutics.

2. Materials and Methods

Animals and TSE Agents

Hamster-adapted scrapie strain 263K was originally obtained from Dr. Richard Kimberlin (SARDAS, Edinburgh, Scotland) and the ME7 mouse-adapted scrapie strain was originally supplied by Dr. Alan Dickinson (ARC and MRC Neuropathogenesis Unit, Edinburgh, Scotland). Both of these scrapie strains were provided by Dr. Richard Carp (NYS Institute for Basic Research, Staten Island, NY). Strains ME7 and 263K were used to infect CD-1 mice and LVG/LAK hamsters (Charles River Breeding Laboratories, Wilmington, MA, USA), respectively. Preparation of inoculum, injection and sacrificing of animals were performed as previously described (Carp and Callahan, 1981; Carp et al., 1990). The mice were observed daily to detect the onset and progression of clinical signs. Behavioral analysis included evaluation for posture, balance, coordination, and the presence of tremors. Brains from sheep infected with scrapie and white-tailed deer infected with CWD were harvested at the time of clinical disease and frozen at -80^{o} C. Brains from uninfected animals were similarly harvested and frozen.

Generation of Monoclonal Antibodies

PK-treated PrP^{Sc}, which consists of the core protein containing amino acids (aa) 90–231 ($PrP_{90–231}$), was isolated from the brains of 263K infected hamsters using a procedure originally reported by Hilmert and Diringer (1984) and modified by Rubenstein et al. (1994). This material was solubilized using guanidine hydrochloride extraction and methanol precipitation as previously described (Kang et al., 2003) and used as the immunogen. $PrP^{-/-}$ mice were immunized and their immune responses monitored by ELISA as previously described (Kascsak et al, 1987). One of the immunized mice was used to produce hybridomas. The mouse received a final immunization of antigen by the intravenous route in phosphate-buffered saline (PBS) 4 days before fusion. Spleen cells were fused to an SP2/0 myeloma cell line expressing reduced levels of cell surface PrP^{C} (Kim et al., 2003). The hybridomas were screened by ELISA as previously described (Kascsak et al., 1987) and the resulting cells were cloned three times by limiting dilution. Large scale Mab production was carried out using disposable bioreactor flasks (Integra Biosciences, Switzerland) and antibody was purified from media using protein G immunoaffinity chromatography (Pierce, Rockford, IL). Protein was determined by the micro BCA protein assay (Pierce) and isotyping was performed using the mouse monoclonal antibody isotyping kit (Pierce). Each of the Mabs was biotinylated using the EZ-link biotinylation kit (Pierce).

Immunoassays

For the preparation of 10% brain homogenates, brain tissues were homogenized in 10 vol. of ice-cold lysis buffer (10 mM Tris-HCl, 150 mM NaCl, 1% Igepal CA-630 (Nonidet P-40), 0.5% deoxycholate, 5 mM EDTA, pH 8.0) in the presence of 1 mM phenylmethylsulfonyl fluoride (PMSF) (if the homogenate was to be treated with PK, PMSF was omitted from the lysis buffer). After centrifugation at 1,000 x g for 10 min, the supernatants were aliquoted and stored at −80° C.

For the indirect ELISA, brain homogenates were centrifuged at 1,000 x g for 2 min. Sodium dodecyl sulfate (SDS) was added to 1 ml of the supernatants to a final concentration of 1%, heated at 100° C for 10 min and centrifuged at 16,000 x g for 5 min. The supernatants were diluted 10-fold in phosphate buffered saline (PBS) and added to 96-well Costar microtiter plates in a volume of 100 μl per well. After incubation overnight at 4°C, the wells were emptied and washed three times with PBST (PBS containing 0.2% Tween 20). Primary antibodies were diluted to 5 μg/ml, 100 μl is added per well, and the plates were incubated at room temperature for 60 min. The wells were then washed three times with PBST. One hundred microliters (1:1000) of goat anti-mouse lgG (Fab fragments) conjugated to alkaline phosphatase (Sigma Chemical Co.) was added to each well and incubated at room temperature for 60 min. The wells were washed three times with PBST followed by the addition of 100 μl PNPP (4-Nitrophenyl phosphate disodium salt hexahydrate, Sigma) substrate solution. The OD_{405} was measured after a 37° C incubation for 60 min.

For the capture ELISA assay, 96-well plates were coated with affinity-purified capture Mab (5 μg/ml) at room temperature for 2–3 hrs. The coated wells were blocked with 3% bovine serum albumin (Sigma) in PBS overnight at 4° C. The wells were washed three times with PBST. The antigen was either non-PK or PK (100 μg/ml PK at 50 °C for 30 min) treated brain lysates to which was added a final concentration of 1% PMSF. All samples were treated with 1% SDS (final concentration), heated at 100° C for 10 min. and centrifuge at 16,000 x g for 5 min. The supernatants were diluted 10-fold and 100 μl was added to each well. The plates were incubated at 37° C for 1 hr. The wells were washed three times with PBST and 100 μl of the biotinylated detector antibody (5 μg/ml) was added. After 60 min the wells were washed with PBST and 100 μl streptavidin conjugated to alkaline phosphatase (!:5,000) was added for 60 min at 37° C. PNPP (4-Nitrophenyl phosphate disodium salt hexahydrate) (Sigma) substrate solution was added to each well (100 μl) and after 60 min, product was measured with an ELISA reader (Bio-Tek, Vermont, NY) at OD_{405}.

In experiments where samples were eluted for Western blot analysis, following the incubation of detection Mab, 1% SDS (final concentration) was added to the wells followed by heating at 100° C for 10 min.

Western Blotting

Ten percent brain homogenates were prepared in lysis buffer as described above. Proteins were subjected to SDS-polyacrylamide gel electrophoresis (SDS-PAGE) using 12% acrylamide gels, transferred to nitrocellulose membranes and immunostained using either streptavidin-conjugated to alkaline phosphatase with NBT and BCIP as the substrate (Kascsak et al., 1986) or horseradish peroxidase-conjugated goat anti-mouse IgG (Pierce) with super signal west femto maximum sensitivity substrate (Pierce) as previously described (LaFauci et al., 2006). For samples that were PK digested prior to SDS-PAGE, treatment involved incubation with 100 μg/ml PK for 30 min at 50° C followed by the addition of 1% PMSF, 1X SDS-PAGE sample buffer and heating at 100° C for 5 min.

3. Results

Numerous Mabs were generated using the solubilized PrP^{Sc} as immunogen and the low PrP expressing SP2/0 myeloma cell line. Three of these Mabs, 08-1/5D6 (5D6), 08-1/11F12 (11F12) and 08-1/8E9 (8E9) were selected for this study and have been isotyped as IgG1, IgG2b and IgG2b respectively. Mapping studies indicated that 5D6 reacts with an, as yet, undefined $PrP_{\sim 90–231}$-specific conformational epitope while 11F12 binds to a region of PrP spanning aa 93–122 and 8E9 reacts within the region of aa 155–200. Individually, all three Mabs react with both the normal and disease associated PrP isoforms.

Western blotting of total brain lysates (Figure 1) demonstrated that all three Mabs were reactive against PrP from non-protease treated brain samples and PK-treated PrP^{Sc} from 263K-infected hamsters, scrapie-infected sheep and CWD-infected deer (Figure 1). Similar results were observed using untreated and PK-treated partially purified PrP^{Sc} preparations (data not shown). These Mabs were also immunoreactive against the normal and abnormal PrP isoforms and PK-treated PrP^{Sc} isolated from mouse brains infected with the ME7, 139A and 22L mouse-adapted scrapie strains and CJD-infected human brain as well as PrP^{C} derived from uninfected brain material from all the species tested including cattle (data not shown). The diglycosylated, monoglycosylated and unglycosylated PrP^{Sc} forms are immunodetected (albeit to different degrees) in all samples regardless of the Mab used. Mabs 5D6 and 8E9 show similar glycosylation patterns of immunostaining with the monoglycosylated band from hamsters and the diglycosylated bands in sheep and deer being the most reactive. Mab 11F12 immunostains the di-and mono-glycosylated hamster PrP similarly while reacting mainly with the diglycosylated sheep PrP and monoglycosylated deer PrP.

By indirect ELISA, the three Mabs were immunoreactive to PK-treated PrP^{Sc} purified from 263K-infected hamster brains. The degree of reactivity was dependent on the extent of the denaturation treatment. Either heat or SDS treatment alone increased immunoreactivity but a combination of the two treatments resulted in the highest levels of antibody binding and immunoreactivity (Table 1) approximating an additive effect of the two treatments and suggesting that epitope exposure is a multi-mechanistic process. Interestingly, although 5D6 binds to a conformational epitope, reactivity of this Mab is not lost, but rather enhanced upon PrP denaturation. It has previously been reported (Tayebi et al., 2004) that heat denaturation is not sufficient to disrupt the polymeric structure of PrP^{Sc}. Furthermore, the Mabs were equally immunoreactive by ELISA to both PrP^{C} from uninfected brains and total PrP (normal and abnormal PrP isoforms)in non-denatured brain homogenate. Immunoreactivity was equally enhanced approximately 2-fold following denaturation with SDS and heat. Following PK treatment and denaturation, the immunoreactivity of PrP^{Sc} was increased an additional 3-fold due to the presence of less exogenous brain protein binding as a result of the proteolytic digestion (data not shown).

To increase specificity and sensitivity for PrP detection, we utilized a capture ELISA assay incorporating a biotinylated detection antibody. As expected, for each of the Mabs biotinylated, 5–6 biotins were bound to each antibody molecule. Further, the biotinylation of the Mabs did not interfere with or reduce their immunoreactivity as assessed by indirect ELISA using partially purified PK-treated PrP^{Sc} (data not shown). Therefore, any differences in the binding and reactivity of the detection antibodies are not the result of the physical biotinylation process. Using PK-treated PrP^{Sc} that had been denatured with SDS and heat, several Mab combinations were examined and each antibody was assessed both as the capture reagent and as the detection reagent (Table 2). Only one of the antibody combinations, Mab 11F12 as the capture reagent and biotinylated 5D6 as the detector, was successful in binding to and identifying PrP^{Sc}. The results were the same regardless of whether the PrP^{Sc} was derived from 263K-infected hamsters, scrapie sheep or CWD-affected deer. The capture ELISA assay utilizing the

11F12-5D6 Mab combination was next assessed for its ability to detect PrP in total and PK-treated brain homogenates from uninfected and infected hamsters, sheep and deer (Figure 2). Similar to the results described above for the indirect ELISA assay on purified hamster brain PrP^{Sc}, the detection of PrP in the capture ELISA assay was also dependent on epitope availability and determined by the initial treatment of brain lysate. Untreated brain lysate from infected animals showed a slight (1.5-fold) increase in signal intensity compared to uninfected brain material whereas either detergent or heat denaturation alone resulted in a 4 to7-fold increase. Not surprisingly, the highest levels (greater than 10-fold) of PrP^{Sc} detection were achieved when a combination of SDS and heat treatment were used. Furthermore, increasing the concentration of SDS above 1% reduced PrP^{Sc} detectability most likely due to an inhibition and/or reversal of antibody-antigen binding. This harsh denaturation treatment, as will be seen below, was not sufficient to completely destroy PrP conformation. It has previously been reported that scrapie infectivity, and presumably some degree of PrP^{Sc} conformation, could be maintained in purified PrP^{Sc} preparations following treatment with SDS, heat and SDS-PAGE (Brown et al., 1990;Rubenstein et al., 1994).

PrP^{C} could be detected in non-PK treated normal brain homogenates by capture ELISA from all three species. In all cases, the signal intensity (~0.25–0.3) was no greater than twice above background (~0.12–0.15). This material was eluted from the wells and examined by Western blotting. In contrast to the results described above where PrP^{C} was detected directly from non-PK-treated brain homogenates, Western blotting of eluted samples resulted only in the detection of IgG light and heavy chains. PrP^{C} was not detectable due to the low levels of bound material. Following PK digestion, ELISA values were reduced to background levels indicating the elimination of PrP^{C}. PrP^{Sc} could readily be detected by the capture ELISA assay in PK-treated brain homogenates from 263K-infected hamsters, sheep scrapie and CWD. Interestingly, capture ELISA assays performed on non-PK treated brain homogenates, which contain both PrP^{C} and PrP^{Sc}, showed signal intensities higher than what could be attributed to the PrP^{C} (determined from the non-PK normal tissue) and PrP^{Sc} (determined from the PK-treated infected tissue) aggregate (Figure 2). It is possible that the increased signal intensity is due to the presence and binding of $sPrP^{Sc}$. An alternative explanation is that the binding of the protein, presumably full-length PrP^{Sc}, to the capture Mab induces a spatial change in the antigen which results in the epitope for the second Mab becoming more accessible. We refer to this process as positive immunocooperativity.

With the given set of Mabs used in this study, the degree of positive immunocooperativity, as shown in Figure 2, was species dependent. PrP^{Sc} from CWD-infected deer showed the greatest levels with a 58% increase in 5D6 binding beyond that calculated solely from the combination of PrP^{C} and PrP^{Sc}, while sheep scrapie PrP^{Sc} showed a 46% increase. PrP^{Sc} from 263K-infected hamsters exhibited the least, but still significant, with 40%.

An antibody-induced spatial rearrangement and/or conformational change in PrP^{Sc} can be demonstrated by showing that the 11F12-5D6 captured material has altered the epitope for another PrP-specific Mab. The capture assay was performed on non-PK-treated, SDS and heat denatured PrP^{Sc}. This was followed by incubation with biotinylated Mab 8E9, streptavidin-alkaline phosphatase and substrate. The lack of a signal above background indicated that the epitope for Mab 8E9 was either no longer available or accessible. However, elution of the 11F12-5D6 captured material from the microtiter wells followed by Western blotting and immunostaining with Mab 8E9 demonstrated robust PrP^{Sc} staining indicating that the Mab 8E9 epitope was once again available (Figure 3). Presumably treatment with SDS-PAGE sample buffer, along with electrophoresis in the presence of SDS, alters the 11F12-5D6 binding to PrP^{Sc} and reverses the antibody-induced PrP^{Sc} changes to once again enable 8E9 binding.

Although Mab 8E9 was able to bind to PrP^{C} and PrP^{Sc} directly on Western blots and indirect ELISA assays, replacing 5D6 with 8E9 in the capture ELISA assay resulted in no detectable PrP indicating the absence of biotinylated 8E9 binding to the antigen. Furthermore, the PrP^{Sc} specificity of the 11F12–5D6 antibody pair was not only due to the presence of these specific Mabs but also to the sequence of the binding events. Reversing the antibodies by utilizing 5D6 as the capture reagent and biotinylated 11F12 as the detection reagent (5D6/Biotin 11F12) resulted in minimal PrP^{Sc} binding from non-PK treated brain lysates when compared to the 11F12-biotinylated 5D6 combination (11F12/Biotin 5D6) (Figure 4). A signal to noise (S/N) ratio was obtained by comparing the PrP signal obtained with the capture assay using infected brain lysates with the variance in the background signal obtained from uninfected material from hamster, sheep and deer brain tissue ($S/N = (S-S_0)/(3\sigma_{S0})$; where S=signal, S_0=mean background signal, σ_{S0} = standard deviation of the background signal). A S/N ratio of less than 1 indicates that a binding of the Mab is sufficiently weak that the signal measured contains a significant amount of noise. On the other hand, a S/N of 1 or greater indicates that the noise in the measurement is not significant indicating that most of the power in the measurement results from specific Mab binding. The confidence level increases exponentially as the S/N ratio increases. For the 5D6/Biotin 11F12 pair, the S/N ratios were approximately 0.6, 0.1 and 0.3 for hamster, sheep and deer, respectively, indicating that the Mab binding was nonspecific. However, with the 11F12/Biotin 5D6 combination the S/N ratios were approximately 19 (hamster), 28 (sheep) and 42 (deer). These ratios are indicative of the highly significant nature of the specific Mab binding.

4. Discussion

The diagnosis of prion diseases, such as scrapie and BSE, has traditionally relied upon the identification of the disease-associated form of the prion protein, PrP^{Sc}, based on its resistance to digestion by PK. Studies have reported on the use of differential solubility with chaotropic agents in the absence of, or in combination with, PK along with phosphotungstic precipitation for the detection of PrP^{Sc} using the time-resolved fluorescence (DELFIA) reporter system (Barnard and Sy, 2003; Dabaghian et al., 2005; Safar et al., 1998, 2002). However, these extraction protocols still suffer from the possibility of selective loss of soluble forms of PrP^{Sc} (Muramoto et al., 1996). A distinct approach, one that circumvents protease digestion, is the conformation-dependent immunoassay (Safar et al., 1998, 2002) that takes advantage of the differential availability of sequestered antibody epitopes between PrP^{C} and PrP^{Sc}. An antibody is used which recognizes a central epitope with differential accessibility between PrP^{C} (available) and PrP^{Sc} (not accessible until thermal or chemical denaturation).

Circumvention of the differential solubilities and protease digestion step might theoretically yield increased sensitivity of PrP^{Sc}-based detection methods and make these methods more amenable to high-throughput technologies. However, it has proved difficult to discriminate between PrP^{C} and PrP^{Sc} with antibodies, despite some early reports (Korth et al., 2003; Paramithiotis et al., 2003; Moroncini et al., 2004). Interestingly, tyrosine-tyrosine-arginine (YYR) motifs (Paramithiotis et al., 2003) were reasoned to be more solvent-accessible in the pathological isoform of PrP, and a monoclonal antibody directed against these motifs was reported to be capable of selectively detecting PrP^{Sc} across a variety of platforms. However, YYR motifs are certainly not unique to pathological prion proteins, and it remains to be determined whether this reagent can really improve the sensitivity of detection of prion infections.

Our studies indicate that antibody binding to PrP in total brain homogenates can induce epitope unmasking. Whether these changes cause PrP conformational alterations, refolding of PrP^{C} into PrP^{Sc} and/or changes in the PK-resistant or $sPrP^{Sc}$ forms to make them more accessible to additional antibody binding is uncertain. Regardless of the mechanism, the dynamics of the

antibody-antigen interaction results in an increase of PrP^{Sc} detection beyond what one would expect from simply an additive effect of the total PrP present. These findings point to the ability to increase the sensitivity of PrP^{Sc} detection without the need to proteolytically digest the PrP^{C}.

Most proteins assume a distinct three-dimensional structure in vivo and in vitro, and this native structure is necessary for function. A protein's structure is determined by its amino acid sequence and the surrounding environment and as a protein unfolds, interactions are disrupted and both secondary and tertiary structure can be lost. In addition, the folded and unfolded states of proteins are in equilibrium. Even under conditions that favor the folded state, a protein is not locked into a single conformation. The amino acids are free to interact and move according to the forces placed on them by neighboring atoms and the solvent, producing many conformations that may differ only very slightly (conformers). Even slight changes in binding epitopes attributable to either localized or more dramatic conformational changes of a protein can have profound effects on antibody-based diagnostic tests. Protein motion can have dramatic effects on protein-protein interactions, specifically antibody-epitope recognition (Kimmermann et al., 2006; Jimenez et al., 2004). For the prion protein, the same amino acid sequence can produce different folded structures, which can hide or create new epitopes. PrP^{Sc} is intrinsically polymorphic and heterogeneous with respect to conformation (Tzaban et al., 2002). Using an array of PrP-specific antibodies, Novitskaya et al (2006) studied the conformation of multimeric PrP within a single fibril or particle without PK pretreatment of the sample on amyloid fibrils prepared from full-length recombinant PrP. This revealed conformational heterogeneity of PrP fibrils as measured for either the entire fibrillar population or even within individual fibrils.

TSE agent pathogenesis and propagation may occur through PrP^{C}-PrP^{Sc} interactions in association with additional macromolecules (nucleic acids, proteins, lipids, etc) resulting in PrP^{Sc} directed conversion of PrP^{C} into new PrP^{Sc}. This process has been modeled in cell-free reactions (Horiuchi et al., 1999, 2001; Kocisko et al., 1994; Saborio et al., 2001). The sequence- and strain-specificities of these reactions suggest that such interactions between the normal and abnormal isoforms play important roles in the propagation and pathogenesis of TSE diseases (Caughey et al., 2001).

It has previously been reported (Li et al., 2000) that binding of Mabs to the N-terminus of recombinant PrP (in the region of aa 23–145) could block the recognition of another antibody that normally binds to a conformational epitope located within the C terminus. The mechanism responsible for this negative immunocooperativity is not clear but probably involves an N-terminus binding-induced conformational change in the C-terminus, resulting in the loss of the C-terminus antibody epitope. Such a conformational change is probably subtle and limited to specific regions of the PrP (Li et al., 2000). In addition, it has been reported that together with the highly flexible aa 90–123 tail, the aa 132–160 PrP segment participates in the structural reorganization to PrP^{Sc} (Torrent et al., 2004). Our studies are in agreement with those findings since 11F12 binds in the region of aa 93–122 and leads to a refolding event resulting in epitope modifications. Furthermore, it is interesting to speculate that although the Mabs in the present study were all raised to PK-treated PrP^{Sc} which is devoid of the first approximately 90 aa at the N-terminus, this region could nevertheless play a role in the full-length PrP^{Sc} positive immunocooperativity we observed following antibody binding at a distant epitope.

The PrP^{Sc}-induced transformation of PrP^{C} into protease-resistant forms can be separated kinetically and biochemically into two different steps: first, the binding between PrP^{C} and PrP^{Sc}, and second, the conversion of the bound PrP^{C} to PrP^{Sc}. Thus, the generation of protease-resistant PrP can be affected either at the binding or conversion steps. Data indicate that the inhibition of PrP^{Sc} formation by the PrP synthetic peptides 109–141, 166–179 and 200–223 is

due to interference with the initial binding between the two PrP isoforms as a result of the peptide directly binding to PrP^{C} (Horiuchi et al., 2001). This binding could physically block the PrP^{Sc} binding site and/or alter the conformation of PrP^{C} making it incapable of binding to PrP^{Sc}. On the other hand, our data using native PrP suggests that targeting other regions of the PrP molecule (i.e. aa 93–122) is likely capable of augmenting the initial PrP^{C}-PrP^{Sc} interaction. Previously, antibody binding studies have suggested that PrP aa residues 90–120 are likely to be critical for the conversion of PrP^{C} to PrP^{Sc} (Peretz et al., 1997). Since the conversion of PrP^{C} to PrP^{Sc} involves conformational changes in the prion protein, it is likely that some of the PrP-specific antibody binding epitopes will be altered. Furthermore, denaturation of $sPrP^{Sc}$ with chaotropes enhances its immunoreactivity toward certain antibodies, due to exposure of partially buried epitopes, which are equally available in native PrP^{C} (Safar et al., 1998). These changes in epitope availability can be used to study the PrP folding/unfolding process during the course of infection and may be used to alter agent propagation. Studies using Mabs have indicated that residues 93–102 are exposed in PrP^{C} but are buried upon conversion to the PrP^{Sc} isoform. Furthermore, PrP103–107 residues are partially buried in PrP^{Sc} while only the PrP107–112 epitope remains exposed, suggesting that the region PrP93–112 undergoes conformational changes during its conversion to PrP^{Sc} (Yuan et al., 2005). Further, studies performed using different combinations of anti-PrP Mabs with mice affected with various mouse-adapted scrapie strains found that some PrP conformational changes, as assessed by PrP antibody epitope availability, could be common while others are specific for the various scrapie strains (Pan et al., 2004).

The infectious agent is detected in lymphoid tissue prior to the onset of clinical signs associated with replication in the central nervous system. Chronic inflammatory conditions involve various cell types of the immune system (including B and T lymphocytes, follicular dendritic cells (FDCs), dendritic cells and macrophages), some of which have been associated with replication of the infectious agent (Kitamoto et al., 1991; Brown et al., 1999; Klein et al., 2001; Prinz et al., 2003). It is possible that these cells might release factors, including antibodies, which induce PrP conformational alterations. In addition, activated B lymphocytes express lymphotoxins which stimulates FDC differentiation and PrP^{C} up-regulation in stromal FDC precursors which, in turn, appear to confer infectious agent replication competence to sites of inflammation in otherwise agent-free organs (Heikenwalder et al., 2005).

Defining the influence of antibody binding on PrP conformational alterations and agent replication would facilitate studies interrogating the entire protein for the sites that are necessary for the conversion process to occur. This, in turn, would have implications into the identification of therapeutic target sites on the protein that could be manipulated to prevent disease progression and subsequent neuropathogenesis..

Acknowledgements

We are appreciative to Dr. Thomas Wisniewski (New York University) for synthetic peptides. This work was supported in part by the National Heart, Lung and Blood Institute (1RO1 HL63837), Health Science Center Research Initiative and US Army Medical Research and Materiel Command (DAMD17-03-1-0368).

References

Abid K, Soto C. Biomedicine and diseases: Review the intriguing prion disorders. Cell Mol Life Sci 2006;63:2342–2351. [PubMed: 16927029]

Alonso DOV, An C, Daggett V. Simulations of biomolecules: characterization of the early steps in the pH-induced conformational conversion of the hamster, bovine, and human forms of the prion protein. Philos Trans R Soc Lond A 2002;360:1–13.

Alonso DOV, DeArmond SJ, Cohen FE, Daggett V. Mapping the early steps in the pH-induced conformational conversion of the prion protein. Proc Natl Acad Sci USA 2001;98:2985–2989. [PubMed: 11248018]

Barnard, G.; Sy, MS. The diagnosis of transmissible spongiform encephalopathies using differential extraction and DELFIA. In: Krull, I., editor. Prions and Mad Cow Disease. Marcel Dekker; New York: 2003. p. 277-315.

Basler K, Oesch B, Scott M, Westaway D, Wälchli M, Groth DF, McKinley MP, Prusiner SB, Weissmann C. Scrapie and cellular PrP isoforms are encoded by the same chromosomal gene. Cell 1986;46:417–428. [PubMed: 2873895]

Brown KL, Stewart K, Ritchie DL, Mabbott NA, Williams A, Fraser H, Morrison WI, Bruce ME. Scrapie replication in lymphoid tissues depends on prion protein-expressing follicular dendritic cells. Nature Med 1999;5:1308–1312. [PubMed: 10545999]

Brown P, Liberski PP, Wolff A, Gajdusek DC. Conservation of infectivity in purified fibrillary extracts of scrapie-infected hamster brain after sequential enzymatic digestion or polyacrylamide gel electrophoresis. Proc Natl Acad Sci USA 1990;87:7240–7244. [PubMed: 2119503]

Carp RI, Callahan SM. In vitro interaction of scrapie agent and mouse peritoneal macrophages. Intervirology 1981;16:8–13. [PubMed: 6799420]

Carp RI, Kim YS, Callahan SM. Pancreatic lesions and hypoglycemia-hyperinsulinemia in scrapie-infected hamsters. JInfect Dis 1990;161:462–466. [PubMed: 2313125]

Carrell RW, Gooptu B. Conformational changes and disease—serpins, prions and Alzheimer's. Curr Opin Struct Biol 1998;8:799–809. [PubMed: 9914261]

Caughey B. Interactions between prion protein isoforms: the kiss of death? Trends Biochem Sci 2001;26:235–242. [PubMed: 11295556]

Caughey B, Raymond GJ. The scrapie-associated form of PrP is made from a cell surface precursor that is both protease- and phospholipase-sensitive. J Biol Chem 1991;266:18217–18223. [PubMed: 1680859]

Caughey B, Raymond GJ, Callahan MA, Wong C, Baron GS, Xiong L. Interactions and conversions of prion protein isoforms. Adv Prot Chem 2001;57:139–169.

Caughey B, Raymond GJ, Ernst D, Race RE. N-Terminal truncation of the scrapie-associated form of PrP by lysosomal protease(s)-implications regarding the site of conversion of PrP to the protease-resistant state. J Virol 1991;65:6597–6603. [PubMed: 1682507]

Cohen FE, Prusiner SB. Pathologic conformations of prion proteins. Ann Rev Biochem 1998;67:793–819. [PubMed: 9759504]

Collins PS, Lawson VA, Masters PC. Transmissible spongiform encephalopathies. Lancet 2004;363:51–61. [PubMed: 14723996]

Cordeiro Y, Kraineva J, Gomes MPB, Lopes MH, Martins VR, Lima LMTR, Foguel D, Winter R, Silva JL. The amino-terminal PrP domain is crucial to modulate prion misfolding and aggregation. Biophys J 2005;89:2667–2676. [PubMed: 16040743]

Dabaghian RH, Barnard G, McConnell I, Clewley JP. An immunoassay for the pathological form of the prion protein based on denaturation and time resolved fluorometry. J Virol Methods 2005;132:85–91. [PubMed: 16219367]

Dickinson AG, Outram GW. Genetic aspects of unconventional virue infections: the basis of the virino hypothesis. Ciba Found Symp 1988;135:63–83. [PubMed: 3044709]

Glatzel M, Ott PM, Linder T, Gebbers JO, Gmür A, Wüst W, Huber G, Moch H, Podvinec M, Stamm B, Aguzzi A. Human prion diseases: epidemiology and integrated risk assessment. Lancet Neurol 2003;2:757–763. [PubMed: 14636781]

Heikenwalder M, Zeller N, Seeger H, Prinz M, Klohn PC, Schwarz P, Ruddle NH, Weissmann C, Aguzzi A. Chronic lymphocytic inflammation specifies the organ tropism of prions. Science 2005;307:1107–1110. [PubMed: 15661974]

Horiuchi M, Baron GS, Xiong LW, Caughey B. Inhibition of interactions and interconversions of prion protein isoforms by peptide fragments from the C-terminal folded domain. J Biol Chem 2001;276:15489–15497. [PubMed: 11279046]

Horiuchi M, Chabry J, Caughey B. Specific binding of normal prion protein to the scrapie form via a localized domain initiates its conversion to the protease-resistant state. EMBO J 1999;18:3193–3203. [PubMed: 10369660]

Jimenez R, Salazar G, Yin J, Joo T, Romesberg FE. Protein dynamics and the immunological evolution of molecular recognition. Proc Natl Acad Sci USA 2004;101:3803–3808. [PubMed: 15001706]

Kascsak RJ, Rubenstein R, Merz PA, Carp RI, Robakis NK, Wisniewski HM, Diringer H. Immunological comparison of scrapie-associated fibrils isolated from animals infected with four different scrapie strains. J Virol 1986;59:676–683. [PubMed: 2426470]

Kascsak RJ, Rubenstein R, Merz PA, Tonna-DeMasi M, Fersko R, Carp RI, Wisniewski HM, Diringer H. Mouse polyclonal and monoclonal antibody to scrapie-associated fibril proteins. J Virol 1987;61:3688–3693. [PubMed: 2446004]

Kim JI, Kuizon S, Rubenstein R. Comparison of PrP transcription and translation in two murine myeloma cell lines. J Neuroimmunol 2003;140:137–142. [PubMed: 12864981]

Kitamoto T, Muramoto T, Mohri S, Doh-Ura K, Tateishi J. Abnormal isoform of prion protein accumulates in follicular dendritic cells in mice with Creutzfeldt-Jakob disease. J Virol 1991;65:6292–6295. [PubMed: 1681118]

Klein MA, Kaeser PS, Schwarz P, Weyd H, Xenarios I, Zinkernagel RM, Carroll MC, Verbeek JS, Botto M, Walport MJ, Molina H, Kalinke U, Acha-Orbea H, Aguzzi A. Complement facilitates early prion pathogenesis. Nature Med 2001;7:410–411. [PubMed: 11283661]

Kocisko DA, Come JH, Priola SA, Chesebro B, Raymond GJ, Lansbury PT, Caughey B. Cell-free formation of protease-resistant prion protein. Nature 1994;370:471–474. [PubMed: 7913989]

Kocisko DA, Priola SA, Raymond GJ, Chesebro B, Lansbury PT Jr, Caughey B. Species specificity in the cell-free conversion of prion protein to protease-resistant forms: a model for the scrapie species barrier. Proc Natl Acad Sci USA 1995;92:3923–3927. [PubMed: 7732006]

Korth C, Stierli B, Streit P, Moser M, Schaller O, Fischer R, Schulz-Schaeffer W, Kretzschmar H, Raeber A, Braun U, Ehrensperger F, Hornemann S, Glockshuber R, Riek R, Billeter M, Wüthrich K, Oesch B. Prion (PrPSc)-specific epitope defined by a monoclonal antibody. Nature 1997;390:74–77. [PubMed: 9363892]

LaFauci G, Carp RI, Meeker HC, Ye X, Kim JI, Natelli M, Cedeno M, Petersen RB, Kascsak R, Rubenstein R. Passage of chronic wasting disease prion into transgenic mice expressing Rocky Mountain elk (*Cervus elaphus nelsoni*) PrP^{C}. J Gen Virol 2006;87:3773–3780. [PubMed: 17098997]

Li R, Liu T, Wong BS, Pan T, Morillas M, Swietnicki W, O'Rourke K, Gambetti P, Surewicz WK, Sy MS. Identification of an epitope in the C terminus of normal prion protein whose expression is modulated by binding events in the N terminus. J Mol Biol 2000;301:567–573. [PubMed: 10966770]

Manuelidis L. A 25 nm virion is the likely cause of transmissible spongiform encephalopathies. J Cell Biochem 2007;100:897–915. [PubMed: 17044041]

Moroncini G, Kanu N, Solforosi L, Abalos G, Telling GC, Head M, Ironside J, Brockes JP, Burton DR, Williamson RA. Motif-grafted antibodies containing the replicative interface of cellular PrP are specific for PrPSc. Proc Natl Acad Sci USA 2004;101:10404–10409. [PubMed: 15240877]

Muramoto T, Scott M, Cohen FE, Prusiner SB. Recombinant scrapie-Like prion protein of 106 amino acids is soluble. Proc Natl Acad Sci USA 1996;93:15457–15462. [PubMed: 8986833]

Novitskaya V, Makarava N, Bellon A, Bocharova OV, Bronstein IB, Williamson RA, Baskakov IV. Probing the conformation of the prion protein within a single amyloid fibril using a novel immunoconformational assay. J Biol Chem 2006;281:15536–15545. [PubMed: 16569635]

Pan KM, Baldwin M, Nguyen J, Gasset M, Serban A, Groth D, Mehlhorn I, Huang Z, Fletterick RJ, Cohen FE, Prusiner SB. Conversion of -helices into β-sheets features in the formation of the scrapie prion proteins. Proc Natl Acad Sci USA 1993;90:10962–10966. [PubMed: 7902575]

Pan T, Li R, Kang SC, Wong BS, Wisniewski T, Sy M-S. Epitope scanning reveals gain and loss of strain specific antibody binding epitopes associated with the conversion of normal cellular prion to scrapie prion. J Neurochem 2004;90:1205–1217. [PubMed: 15312175]

Paramithiotis E, Pinard M, Lawton T, LaBoissiere S, Leathers VL, Zou WQ, Estey LA, Lamontagne J, Lehto MT, Kondejewski LH, Francoeur GP, Papadopoulos M, Haghighat A, Spatz SJ, Head M, Will R, Ironside J, O'Rourke K, Tonelli Q, Ledebur HC, Chakrabartty A, Cashman NR. A prion protein

epitope selective for the pathologically misfolded conformation. Nature Med 2003;9:893–899. [PubMed: 12778138]

Peretz D, Williamson RA, Matsunaga Y, Serban H, Pinilla C, Bastidas RB, Rozenshteyn R, James TL, Houghten RA, Cohen FE, Prusiner SB, Burton DR. A conformational transition at the N terminus of the prion protein features in formation of the scrapie isoform. J Mol Biol 1997;273:614–622. [PubMed: 9356250]

Prinz M, Heikenwalder M, Junt T, Schwarz P, Glatzel M, Heppner FL, Fu YX, Lipp M, Aguzzi A. Positioning of follicular dendritic cells within the spleen controls prion neuroinvasion. Nature 2003;425:957–962. [PubMed: 14562059]

Prusiner SB. Novel proteinaceous infectious particles cause scrapie. Science 1982;216:136–144. [PubMed: 6801762]

Prusiner SB. Prions. Proc Natl Acad Sci USA 1998;95:13363–13383. [PubMed: 9811807]

Rubenstein R, Carp RI, Ju W, Scalici C, Papini M, Rubenstein A, Kascsak R. Concentration and distribution of infectivity and PrPSc following partial denaturation of a mouse-adapted and a hamster-adapted scrapie strain. Arch Virol 1994;139:301–311. [PubMed: 7832637]

Safar JG, Geschwind MD, Deering C, Didorenko S, Sattavat M, Sanchez H, Serban A, Vey M, Baron H, Giles K, Miller BL, DeArmond SJ, Prusiner SB. Diagnosis of human prion disease, Proc. Natl Acad Sci USA 2005;102:3501–3506.

Safar JG, Scott M, Monaghan J, Deering C, Didorenko S, Vergara J, Ball H, Legname G, Leclerc E, Solforosi L, Serban H, Groth D, Burton DR, Prusiner SB, Williamson RA. Measuring prions causing bovine spongiform encephalopathy or chronic wasting disease by immunoassays and transgenic mice. Nature Biotechnol 2002;20:1147–1150. [PubMed: 12389035]

Safar J, Wille H, Itri V, Groth D, Serban H, Torchia M, Cohen FE, Prusiner SB. Eight prion strains have $PrP^{(Sc)}$ molecules with different conformations. Nature Med 1998;4:1157–1165. [PubMed: 9771749]

Saborio GP, Permanne B, Soto C. Sensitive detection of pathological prion protein by cyclic amplification of protein misfolding. Nature (London) 2001;411:810–813. [PubMed: 11459061]

Stahl N, Baldwin MA, Teplow DB, Hood L, Gibson BW, Burlingame AL, Prusiner SB. Structural studies of the scrapie prion protein using mass spectrometry and amino acid sequencing. Biochemistry 1993;32:1991–2002. [PubMed: 8448158]

Stahl N, Prusiner SB. Prions and prion proteins. FASEB J 1991;5:2799–2807. [PubMed: 1916104]

Tayebi M, Enever P, Sattar Z, Collinge J, Hawke S. Disease-associated prion protein elicits immunoglobulin M responses in vivo. Mol Med 2004;10:104–111. [PubMed: 15706401]

Torrent J, Alvarez-Martinez MT, Liautard JP, Balny C, Lange R. The role of the 132–160 region in prion protein conformational transitions. Prot Sci 2004;14:956–967.

Tzaban S, Friedlander G, Schonberger O, Horonchilk L, Yedidia Y, Shaked G, Gabizon R, Taraboulos A. Protease-sensitive scrapie prion protein in aggregates of heterogeneous sizes. Biochemistry 2002;41:12868–12875. [PubMed: 12379130]

Wadsworth JDF, Collinge J. Update on human prion disease. Biochim Biophys Acta 2007;1772:598–609. [PubMed: 17408929]

Yuan FF, Biffin S, Brazier MW, Suarez M, Roberto CC, Hill A, Collins SJ, Sullivan JS, Middleton D, Multhaup G, Geczy AF, Masters CL. Detection of prion epitopes on PrPc and PrPsc of transmissible spongiform encephalopathies using specific monoclonal antibodies to PrP. Immunol Cell Biol 2005;83:632–637. [PubMed: 16266315]

Zimmermann J, Oakman EL, Thorpe IF, Shi X, Abbyad P, Brooks CL III, Boxer SG, Romesberg FE. Antibody evolution constrains conformational heterogeneity by tailoring protein dynamics. Proc Natl Acad Sci USA 2006;103:13722–13727. [PubMed: 16954202]

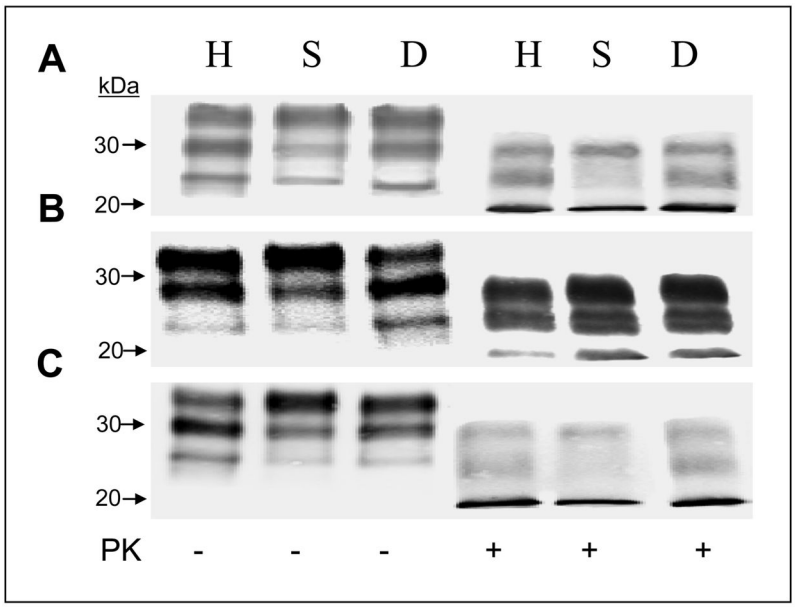

Figure 1.
Western blot analysis of untreated and PK treated total brain lysates from 263K-infected hamsters (H), scrapie-infected sheep (S) and CWD-infected deer (D) using Mabs 08-1/5D6 (A), 08-1/11F12 (B), and 08-1/8E9 (C).

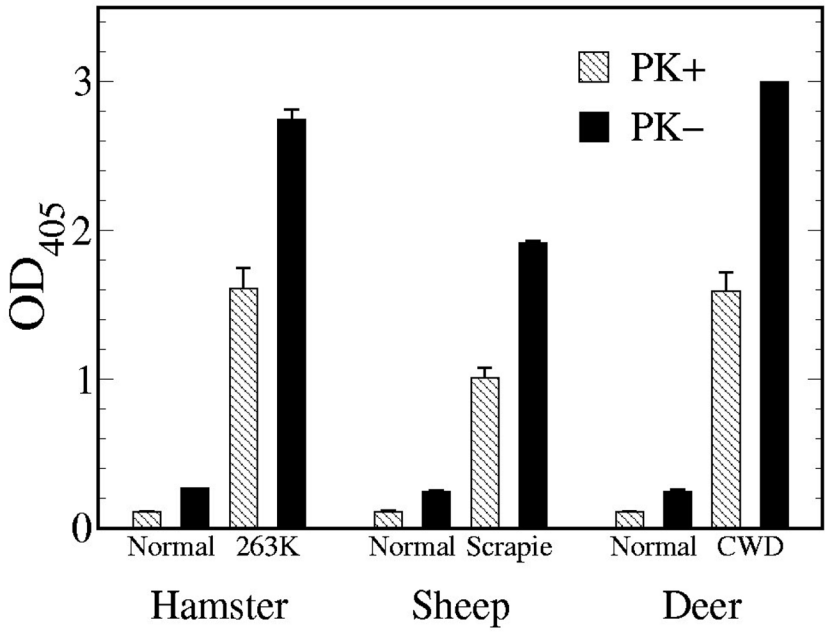

Figure 2.

Capture ELISA assay using Mabs 11F12 as the capture reagent and biotinylated 5D6 as the detection reagent. Brain tissue homogenates from normal and infected hamsters, sheep and deer were prepared as described in Materials and Methods. The capture ELISA assay was performed on non-PK and PK-treated brain lysates. Antibody binding was measured colorimetrically at OD_{405}. Each value is based on triplicate readings for six individual samples for each species and expressed as the mean ± standard deviation.

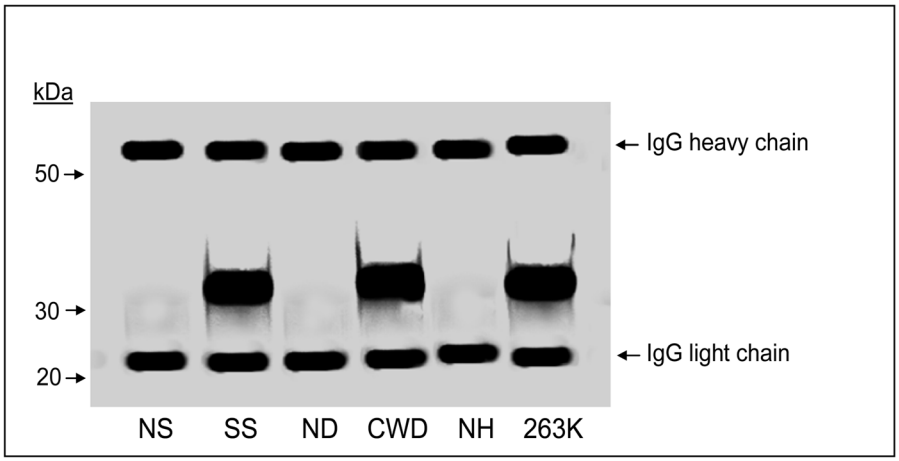

Figure 3.

Western blot analysis of non-PK treated brain homogenates following capture ELISA assay. The capture ELISA assay was carried out on normal sheep (NS), scrapie-infected sheep (SS), normal deer (ND), CWD-infected deer (CWD), normal hamster (NH) and 263K-infected hamsters (263K) under the same conditions as described for Figure 2 using a non-biotinylated detection reagent. The material was eluted from the microtiter plate as described in Materials and Methods and Western blotted. Immunostaining was carried out using Mab 8E9.

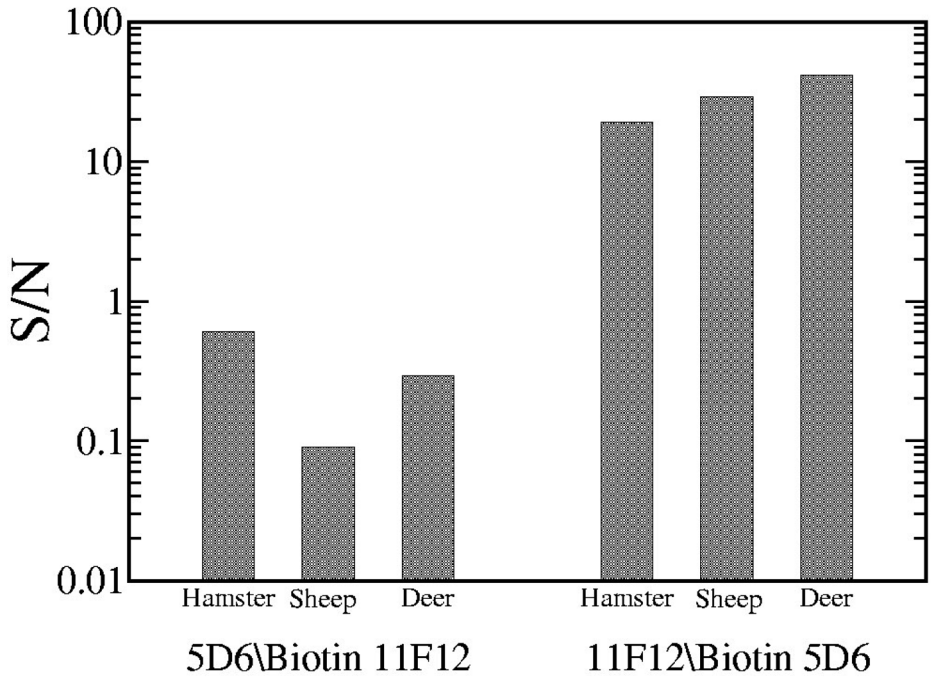

Figure 4.

Comparison of reversing the capture and detection reagents in the capture ELISA assay using brain lysates from uninfected and infected hamsters, sheep and deer. Studies using 5D6 as the capture reagent and 11F12 as the biotinylated detection reagent (5D6/Biotin 11F12) are compared to using 11F12 as the capture reagent and 5D6 as the biotinylated detection reagent (11F12/Biotin 5D6). Each assay was performed in triplicate on six individual samples for each species and the ELISA results calculated as the mean ± standard deviation. The increased antibody binding from infected samples (based on the OD_{405}) are compared to the uninfected controls. Plotted on a logarithmic scale is the signal to noise ratio (S/N) as calculated from the signal power of the infected samples to the power in the control samples (noise).

Table 1

Comparision of Denaturation Treatments on PrP^{Sc} Immunoreactivity[1].

Treatment	Signal Intensity[2]		
	5D6	11F12	8E9
Untreated	0.214 ± 0.017	0.339 ± 0.009	0.303 ± 0.110
SDS[3]	1.229 ± 0.019	1.599 ± 0.182	1.324 ± 0.251
Heat[4]	1.228 ± 0.018	1.085 ± 0.124	1.427 ± 0.331
SDS + Heat	2.232 ± 0.008	2.548 ± 0.112	2.821 ± 0.252

[1] PrP^{Sc} was purified from the brains of clinical hamsters infected with the hamster adapted 263K scrapie strain and PK treated as described in Materials and Methods.

[2] Signal intensity was measured by indirect ELISA assay at OD_{405}.

[3] SDS was added to a final concentration of 1%.

[4] Samples were heated at 100^{o} C for 5 min.

Table 2

Analysis of Mab Pairs for Capture ELISA Assay[1].

Capture Mab	Detection Ab (biotinylated)		
	11F12	5D6	8E9
11F12	−	+	−
5D6	−	−	−
8E9	−	−	−

[1] Mab pairs were analyzed using PK-treated PrP^{Sc} purified from 263K-infected hamster brains. PrP^{Sc} was treated with SDS and heat prior to the capture ELISA assay. All Mabs were diluted to a concentration of 5 μg/ml before use.